MEDICINAL CHEMISTRY RESEARCH

CrossMark

ORIGINAL RESEARCH

Novel adefovir mono L-amino acid ester, mono bile acid ester derivatives: Design, synthesis, biological evaluation, and molecular docking study

Ya Chen[1] · Wen Zheng Zhang[1] · Jing Li[1] · Tao Xiao[1] · Jiang Xia Liu[2] · Min Luo[1] ·
Hang Su[1] · Xiao-Zhong Fu[1] · Ting Liu[3] · Yong-Xi Dong[1] · Yong-Long Zhao[1] · Bin He[3] ·
Yong-Jun Li[3]

Abstract A series of adefovir mono L-amino acid ester, mono bile acid ester derivatives was designed and synthesized. The newly designed compounds have potent anti-anti-hepatitis B activity, especially compound **6c**, which has more potent antiviral activity and a higher selectivity index (EC$_{50}$ 0.65 µmol/L, SI 582.24) than adefovir dipivoxil. Uptake of compounds **6a–f** into rat primary hepatocytes was 71.56, 63.92, 142.88, 104.25, 67.84, and 39.95-fold, respectively, higher than that of adefovir dipivoxil. In the presence of Na$^+$, uptake of compounds **6a–c** by Na$^+$/taurocholate co-transporting polypeptide-Human embryonic kidney 293 cells was 128.5, 137.2 and 121.7-fold higher than that of adefovir dipivoxil. Potential binding modes of compounds **6a** and **6c** to human apical Na$^+$-dependent bile acid transporter were also investigated.

Ya Chen and Wen Zheng Zhang contribute equally to this work.

✉ Xiao-Zhong Fu
   2660860532@qq.com

✉ Ting Liu
   1586740@qq.com

1 School of Pharmacy, Engineering Research Center for the Development and Application of ethnic Medicines and TCM, Ministry of Education, Guizhou Medical University, Guiyang 550004, China

2 Key Laboratory of Medical Molecular Viology, Institute of Medical Microbiology, Shanghai Medical College, Fudan University, Shanghai 200032, China

3 Provincial Key Laboratory of Pharmaceutics in Guizhou Province, Guiyang 550004, China

Introduction

Hepatitis B virus (HBV), a member of the family Hepadnaviridae, is a causative agent, frequently leading to acute and chronic infections in humans (Gitlin 1997). According to the World Health Organization, about 2 billion people world-wide are currently infected with HBV and more than 350 million are chronically infected carriers. The sequelae of acute or chronic HBV infection are estimated to cause the deaths of 800,000 people every year worldwide (Revill and Locarnini 2016). Nucleoside or nucleotide analogs are currently available to treat chronic HBV infection (Jarvis and Faulds 1999; You and Jia 2013; Quan and Peters 2004; Fung et al. 2008), but development of resistance limits their clinical application. Adefovir dipivoxil (AD, Hepsera®), a prodrug that is converted rapidly into the parent drug 9-(2-phosphonomethoxyethyl)adenine (PMEA, adefovir) in vivo, can suppress replication of HBV that is resistant to nucleoside analogs, such as lamivudine, emtricitabine, and famciclovir (Raney et al. 2003; Yuen and Lai 2004). Dose-limiting nephrotoxicity, manifesting as acute tubular necrosis and Fanconi syndrome, together with the potential to release carcinogenic formaldehyde and toxic pivalic acid have, however, restricted the clinical use of adefovir dipivoxil (Valle and Haragsim 2006; Law et al. 2013). Novel anti-HBV agents, based on adefovir but with increased antiviral activity and reduced off-target toxicity, would thus have significant clinical potential.
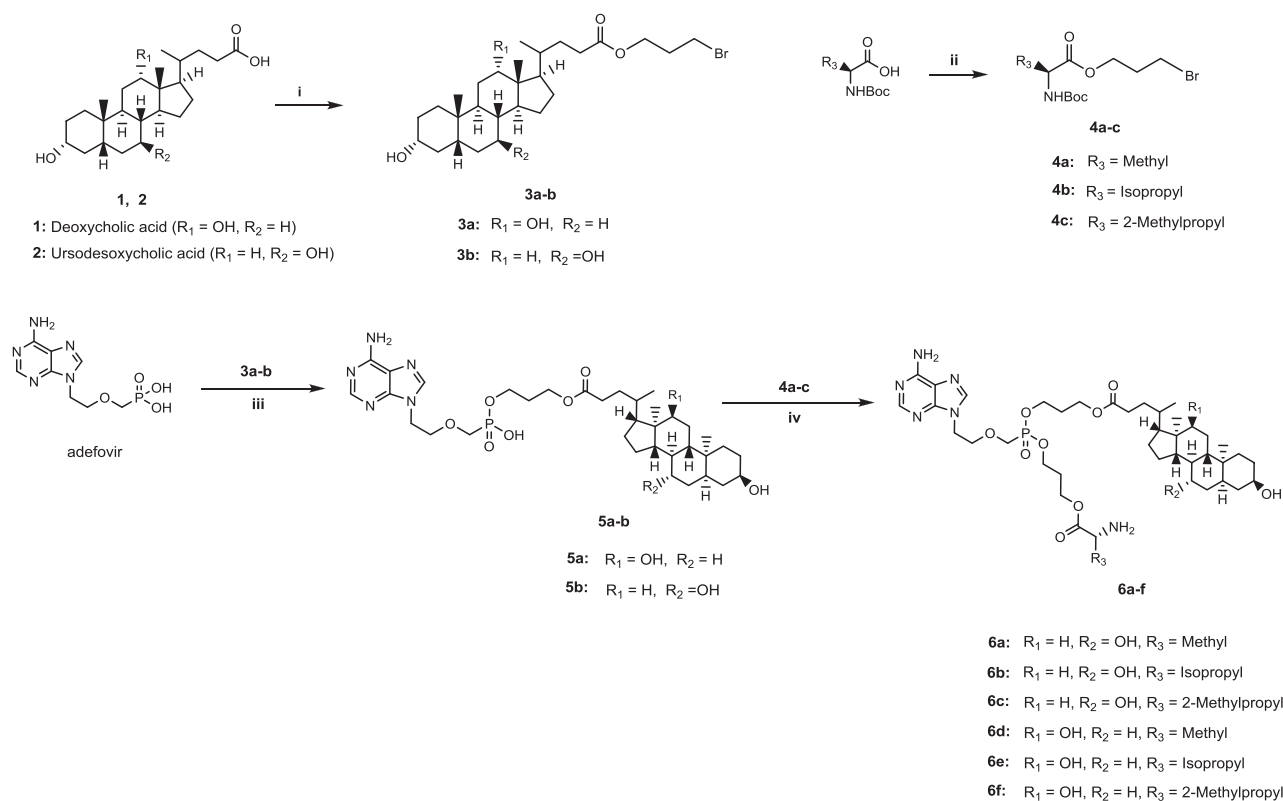
 Springer

Scheme 1 Reagents and conditions: (i) 3-bromo-1-propanol, DCC, DMAP, anhydrous THF, 40 °C, 24 h, yield 56–62% ; (ii) 3-bromo-1-propanol, DCC, DMAP, CH$_2$Cl$_2$, 0 °C-rt, 12 h, yield 84–89%; (iii) *N*,

N-dicyclohexyl-4-morpholine carboxamidine (DCMC), anhydrous DMF, 40–50 °C,48 h; (iv) DCMC, anhydrous DMF, 80–85 °C,48 h, then 60%H$_3$PO$_4$/CHCl$_3$ rt, 6 h, yield 14.5–21.8%

It has been confirmed that bile acids, the acidic sterols commonly existing in bile, physiologically undergo the enterohepatic circulation. This process requires Na$^+$-dependent bile acid transport systems such as human apical Na$^+$-dependent bile acid transporter (hASBT) and Na$^+$/taurocholate co-transporting polypeptide (NTCP), which are localized in the membranes of terminal ileum epithelial cells and hepatocytes, respectively (Schaap et al. 2014; Balakrishnan and Polli (2006). The organotropism of bile acids in the enterohepatic circulation indicates that bile acid-drug conjugates might specifically deliver drugs to the liver, thus reducing undesired side-effects in other organs or tissues, and improve the intestinal absorption of poorly absorbed drugs through bile acid transport systems (Vicens et al. 2007). This prodrug design strategy has been successfully used to increase hepatic targeting and oral bioavailability of chlorambucil, ferulic acid, and gabapentin (Kullak-Ublick et al. 1997; Fiorucci et al. 2003; Rais et al. 2011).

In previous studies, we have designed and synthesized both bis(L-amino acid) ester and mono L-amino acid ester, mono non-steroidal anti-inflammatory drug carboxylic ester prodrugs of adefovir that had enhanced antiviral activity and selectivity index (SI) (Fu et al. 2007; Fu et al. 2012). In the present work, searching for compounds with more potent

anti-HBV activity and sufficient enrichment in the liver, we have adopted a sub-structure combination principle to design mixed adefovir prodrugs formed by esterification of the phosphonic acid moiety with bile acids and L-amino acids. The bioactivity of these mixed prodrugs was evaluated in a range of cellular assays.

Results and discussion

Synthesis

The general procedure for the synthesis of mono L-amino acid ester, mono bile acid ester derivatives of adefovir (**6a–f**) is outlined in Scheme 1. Deoxycholic acid (**1**) and ursodesoxycholic acid (**2**) were converted into 3-bromo-1-propyl esters (**3a**, **3b**) by treatment with 3-bromo-1-propanol in the presence of dicyclohexylcarbodiimide/ 4-dimethylaminopyridine (DCC/DMAP) at 40 °C. Condensation of *N*-Boc L-amino acids, such as alanine (Ala), valine (Val) and isoleucine (Ile), with 3-bromo-1-propanol using DCC/DMAP as condensing agent at low temperature (0 °C to room temperature) provided the corresponding 3-bromo-1-propyl esters (**4a–c**). The activated esters were

then coupled with adefovir using a "one-pot synthesis" method. Compounds **3a** and **3b** were first reacted with adefovir, in the presence of N,N'-dicyclohexyl-4-morpholinecarboxamidine (DCMC) as an acid scavenger, in anhydrous dimethyl formamide (DMF)at 40–50 °C for 48 h, yielding mono bile acid esters of adefovir (**5a**, **5b**). The mono bile esters were not isolated from the mixture but, when the yields were judged to be highest, intermediates **4a–c** were added to the mixture and the reaction temperature was increased to 80–85 °C for 48 h. The solvents were then removed in vacuo, and the mono N-Boc L-amino acid ester, mono bile acid ester prodrugs of adefovir were isolated by flash column chromatography. The N-Boc protecting groups were then removed using 60% H_3PO_4 to provide the target compounds **6a–f**, with total yields in the range 14.5–21.8%. The structures of the compounds were confirmed using $^1H/^{13}C$ nuclear magnetic resonance (NMR), electrospray ionization-mass spectrometry (MS (ESI)) as well as high resolution mass spectrometry (HRMS) (ESI). Spectral data were in accordance with the assigned structures and all characterization data are provided in the experimental section.

Evaluation of anti-HBV activity

The inhibitory effects of the compounds on HBV replication were tested in HepG 2.2.15 cells. All compounds demonstrated anti-HBV activity, with EC_{50} values in the range 0.65–44.13 µmol/L (Table 1). Compounds **6a–c** showed the best antiviral activity, with EC_{50} values in the range 0.65–5.44 µmol/L. Compound **6c** had better antiviral activity (EC_{50} 0.65 µmol/L) and a higher SI (582.24) than AD (EC_{50} 3.09 µmol/L, SI 142.04). Preliminary structure–activity relationship analysis revealed that compounds with ursodesoxycholic acid ester groups (**6a–c**) had higher antiviral activity and selectivity index (EC_{50}

0.65–5.44 µmol/L, SI 89.97–582.24) than compounds with deoxycholic acid ester groups (**6d–f**) (EC_{50} 11.25–44.13 µmol/L, SI 76.95–51.95). Comparison of compounds **6a–c** and **6d–f** indicated that compounds incorporating amino acids with bulky alkyl groups had higher anti-HBV activity and SI than corresponding compounds incorporating amino acids with less bulky alkyl groups.

Uptake into rat primary hepatocytes

Rat primary hepatocytes were cultivated between two layers of collagen (sandwich culture). This type of culture preserves both liver-specific functions and morphology over prolonged periods of time (Dunn et al. 1989; Bader et al. 1992). Based upon above reasons we isolated rat primary hepatocytes by using the two step collagenase perfusion method (La Brecque and Howard 1976), which is essential for the evaluation of uptake in comet assays.

The cellular uptake of compounds **6a–f** was evaluated in rat primary hepatocytes (Figs. 1 and 2). Cellular uptake values of compounds **6a–f** were 99.95 ± 6.96 to 355.79 ± 18.90 µmol min^{-1}(mg of protein)$^{-1}$, which were significantly higher than that of AD (2.49 ± 0.18 µmol min^{-1}(mg of protein)$^{-1}$). Hepatocyte uptake values of compounds **6a–f** were 71.56, 63.92, 142.88, 104.25, 67.84, and 39.95-fold higher, respectively, than that of AD. At 355.79 ± 18.90 µmol min^{-1}(mg of protein)$^{-1}$, compound **6c** had the highest uptake value (Fig. 1). Addition of deoxycholic acid (100 µM) significantly antagonized cellular uptake of compounds **6a–f** (178.18 ± 12.94, 159.17 ± 10.93, 355.79 ± 18.90, 259.59 ± 17.94, 168.93 ± 10.92, and 99.95 ± 6.96 µmol min^{-1}(mg of protein)$^{-1}$, respectively, without deoxycholic acid and 27.08 ± 2.07, 23.77 ± 1.80, 29.88 ± 2.64, 60.74 ± 5.19, 30.15 ± 2.30, and 25.17 ± 1.98 µmol min^{-1}(mg of protein)$^{-1}$, respectively, in the presence

Table 1 Anti-HBV activities of mono L-amino acid ester, mono bile acid ester prodrugs of adefovir

Compound	EC50[a] (µmol/L)	CC50[b] (µmol/L)	SI[c]
6a	5.44	489.48	89.97
6b	3.34	406.68	121.76
6c	0.65	378.46	582.24
6d	44.13	2292.77	51.95
6e	21.46	1447.33	67.44
6f	11.25	865.70	76.95
AD	3.09	438.92	142.04

[a] Concentration of compound achieving 50% inhibition of cytoplasmic HBV DNA synthesis

[b] Concentration of compound required for 50% extinction of HepG2 2.2.15 cells
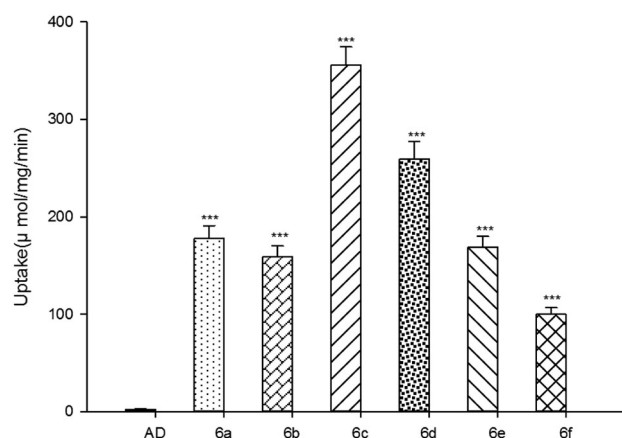
[c] Selectivity index (CC50/EC50)

Fig. 1 Uptake of compounds (**6a–f**) and AD (50 µM) after cultivation for 60 min in rat primary hepatocytes (mean ± SD, $n = 3$), ***$p < 0.001$ compared with AD
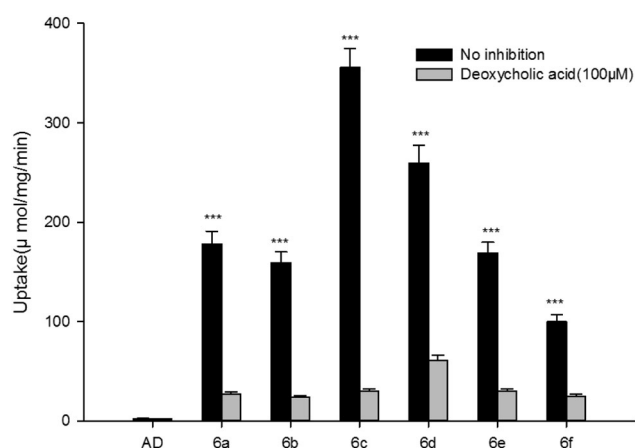
Fig. 2 Uptake of compounds (**6a–f**) and AD (50 μM) in the absence (black bar) of deoxycholic acid or in the presence (grey bar) of deoxycholic acid (100 μM) after cultivation for 60 min in rat primary hepatocytes (mean ± SD, $n = 3$), ***$p < 0.001$, added deoxycholic acid group vs. no added deoxycholic acid group

of deoxycholic acid) (Fig. 2). These results suggest that the bile acid carrier might be involved in recognition, as well as transport, of the hepatotrophic compounds **6a–f**.

Uptake into NTCP-Human embryonic kidney (HEK)293 cells

NTCP (SLC10A1), located on the basolateral membrane of hepatocytes, and is responsible for over 80% of conjugated bile acid uptake into hepatocytes (Kullak–Ublick et al. 2004). HEK293 cells were generated by transformation of cultures of normal human embryonic kidney cells with sheared adenovirus DNA. HEK293 cells are straightforward to grow in culture and to transfect. Based upon above results, we established NTCP-HEK293 cells and to further evaluate uptake for target compounds.

The exact transport mechanism of the adefovir bile acid conjugates, **6a–c**, was further evaluated by examining uptake in NTCP-HEK293 cells. Concentration-dependent uptake of the potential prodrugs into NTCP-HEK 293 monolayers is shown in Fig. 3. Uptake of compounds **6a–c** was greater in the presence of Na^+ than in the absence of Na^+ (panels a, b, c), indicating active uptake by the transporter. Uptake results of AD and positive control taurocholic acid (TA) in the presence of Na^+ and in the absence of Na^+ were provided as (panels d, e), and the results indicating that target compounds exhibit similar transportation amounts and tendency to TA, they are all substrates of NTCP, however AD is not a substrate of NTCP.

Self-inhibition experiments in the presence and absence of Na^+ were also performed using NTCP-HEK293 cells (Table 2). Michaelis–Menten constants (K_m) values for uptake of **6a–c** in the presence of Na^+ (22.71 ± 0.61 to 81.17 ± 5.96 μM) were significantly higher than in

the absence of Na^+ (6.01 ± 0.41 to 12.89 ± 0.48 μM). Maximum uptake velocities (V_{max}) for compounds **6a–c** in the presence of Na^+ were 227.98 ± 15.58, 187.03 ± 13.87 and 593.74 ± 70.34 μmol min^{-1}(mg of protein)$^{-1}$, which were 149.98, 123.04 and 390.62-fold higher, respectively, than the V_{max} value of AD (1.52 ± 0.11 μmol min^{-1}(mg of protein)$^{-1}$). Values of V_{max}/K_m for **6a–c** in the presence of Na^+ were 7.71 ± 0.54, 8.23 ± 0.40 and 7.30 ± 0.33 μL min^{-1}(mg of protein)$^{-1}$, which were 128.5, 137.2 and 121.7-fold, respectively, higher than that of AD (0.06 ± 0.001 μL min^{-1}(mg of protein)$^{-1}$). Values of V_{max}/K_m for **6a–c** in the absence of Na^+ were 153.0, 73.8 and 101.4-fold higher than that of AD (0.05 ± 0.001 μL min^{-1}(mg of protein)$^{-1}$). Taken together, these results indicate that, in the absence of Na^+, the ratios of uptake of prodrugs **6a–c** to that of AD were 73.8–153.0%, indicating that the passive permeability of the prodrugs is >70-fold higher than that of AD. In the presence of Na^+, the ratios of uptake of prodrugs **6a–c** to that of AD were 128.5, 137.2, and 121.7, indicating that translocation via NTCP further enhances uptake of the prodrugs, relative to that of AD. Moreover the obtained kinetic parameters in Table 2 suggesting that transporting capacity of target compounds **6a–c** were relative lower than that of positive control TA in the presence of Na^+.

Molecular docking studies

Possible binding modes of the adefovir mono bile acid ester, mono L-amino acid ester prodrugs with the bile acid transporter were explored by docking compounds **6a** and **6c** into the hASBT binding cleft, using the X-ray crystallographic structure of hASBT (PDB code: 3ZUX). Compound **6c** occupied the bile acid-binding site of hASBT and was held in place by four hydrogen bonds and two hydrophobic bonds (right part of Fig. 4). The hydroxyl group at the 3-position of the bile acid ester fragment of compound **6c** formed two essential hydrogen bonds with Ser-266 and Ser-291, the hydrogen atom at the 6-position of the bile acid ester fragment formed a hydrogen bond with Ile-203 and the hydrogen atom of the 3-methylpropyl group attached to the L-amino acid fragment served as a H-bond donor for Gly-12. In addition to these H-bond interactions, the alkyl group on the five-membered ring of the bile acid group inserted into a small hydrophobic pocket and generated substantial hydrophobic contacts with Phe-15. The purine ring of compound **6c** simultaneously moved to the outer surface and generated a hydrophobic interaction with Pro-196, contributing to its favorable binding affinity. In the case of compound **6a** (left part of Fig. 4), however, the alkoxide phosphonate group had to move away from the neighboring residue to avoid an unfavorable contact. The hydrophobic interaction with residue Pro-196 was lost because of the concerted movement of the whole molecule and potency
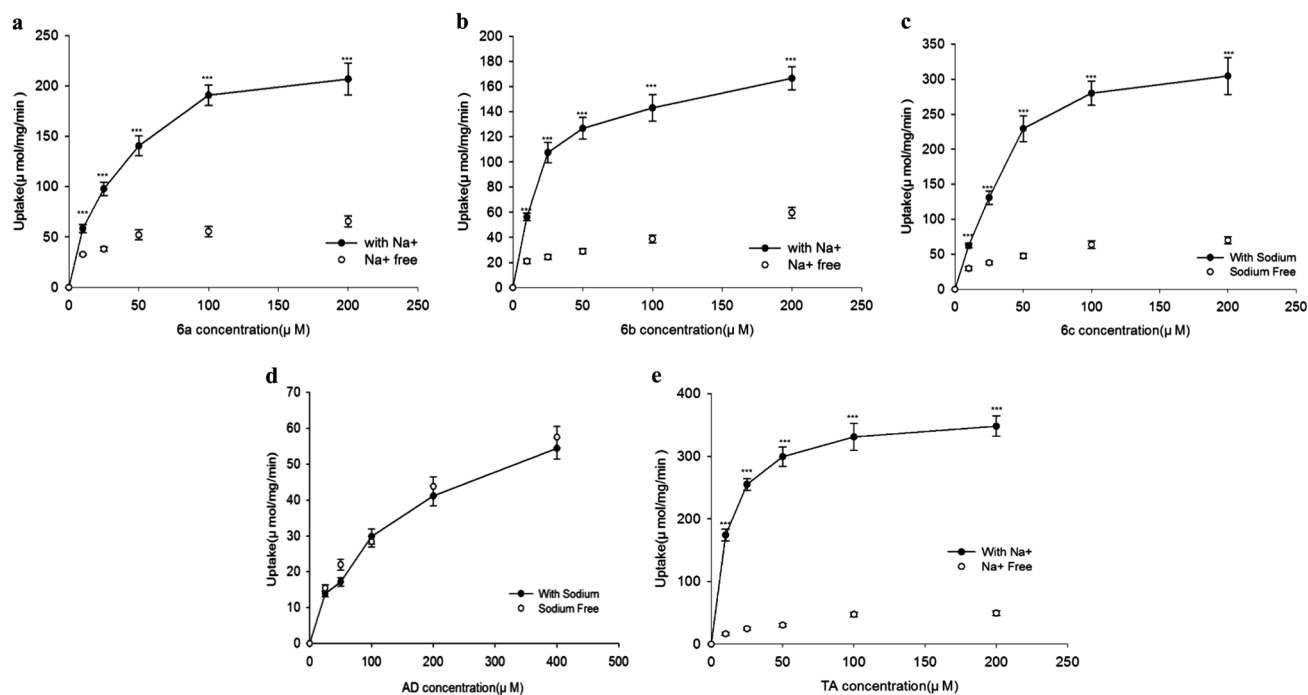
Fig. 3 Concentration-dependent uptake of target compounds **6a–c**, AD and positive control taurocholic acid (TA) into NTCP-HEK 293 cell monolayers. Panels **a**, **b**, and **c** show uptake of compounds **6a**, **6b**, and **6c** in the presence (•) or absence of Na⁺ (°) in NTCP-HEK 293 cell monolayers. Panel **d** and **e** show uptake of AD and TA in the presence (•) or absence (°) of Na⁺ in NTCP- HEK 293 monolayers. ***$p < 0.001$, uptake of compounds in the presence vs. in absence of Na⁺

Table 2 Kinetic parameters for uptake of compounds **6a–c** and AD in NTCP-HEK293 cells in the presence or absence of Na⁺ ($x \pm s$, $n = 3$)

	Na⁺(+)			Na⁺(−)		
	K_m [μM]	V_{max} [μmol min⁻¹(mg of protein)⁻¹]	V_{max}/K_m [μL min⁻¹(mg of protein)⁻¹]	K_m [μM]	V_{max} [μmol min⁻¹(mg of protein)⁻¹]	V_{max}/K_m [μL min⁻¹(mg of protein)⁻¹]
6a	29.58 ± 0.10	29.58 ± 0.10	7.71 ± 0.54	6.01 ± 0.41	46.06 ± 4.20	7.65 ± 0.17
6b	22.71 ± 0.61	22.71 ± 0.61	8.23 ± 0.40	11.46 ± 0.45	42.20 ± 2.84	3.69 ± 0.39
6c	81.17 ± 5.96	81.17 ± 5.96	7.30 ± 0.33	12.89 ± 0.48	65.13 ± 4.42	5.07 ± 0.53
AD	25.28 ± 0.28	1.52 ± 0.11	0.06 ± 0.01	30.80 ± 1.96	1.47 ± 0.12	0.05 ± 0.01
TA	17.16 ± 10.67	318.90 ± 81.81	24.67 ± 14.78	34.31 ± 15.19	72.29 ± 20.37	2.23 ± 0.52

The uptake of target compounds **6a–c**, AD and TA into NTCP-HEK293 cells were measured in the presence or absence of Na⁺. Kinetic parameters were obtained by fitting the one-saturable or one-nonsaturable model as described in experimental section. Data were represented as mean ± SD

was thus reduced. As a result, compound **6a** formed three essential hydrogen bonds with Asn-265 and Asn-295, and generated substantial hydrophobic contacts with Phe-15. These results confirmed our strategy for designing adefovir mono L-amino acid ester, mono bile acid ester derivatives as substrates of bile acid transporter to enhance hepatic targeting of the target compounds.

Conclusion

A series of mono L-amino acid ester, mono bile acid ester derivatives of adefovir (**6a–f**) have been designed and synthesized using a 'one pot synthesis' method. All new compounds were characterized by ¹H/¹³C NMR, ESI–MS and ESI–HRMS. Compounds **6a–c** were shown to have potent anti-HBV activity, especially compound **6c**, which had more potent antiviral activity and a higher selectivity index (EC₅₀ 0.65 μmol/L, SI 582.24) than AD. The uptake of compounds **6a–f**, especially compound **6c**, into rat primary hepatocytes was significantly higher than that of AD. The significantly higher uptake of the newly designed compounds in NTCP-HEK293 cells could be attributed to recognition and transport by the NTCP carrier, suggesting that the compounds are substrates for NTCP. Molecular docking studies revealed potential binding modes of

compounds **6a** and **6c** with hASBT. Overall, our study suggests that the use of a mono L-amino acid ester, mono bile acid ester prodrug strategy is an effective method for designing novel prodrugs of adefovir, which have enhanced antiviral activity and hepatotrophic properties.

Experimental

General. Ursodesoxycholic acid and deoxycholic acid 3-bromo-1-propyl esters (**3a–b**) and *N*-Boc L-amino acid 3-bromo-1-propyl esters (**4a–c**) were prepared according to literature procedures (Fu et al. 2012). Other chemicals were 97–99% pure and were purchased from Sinopharm Chemical Reagent Co, Ltd. (SCRC). ^{1}H/^{13}C NMR spectra (reference tetramethylsilane for δ H, *J* values are given in Hz) were recorded using a Varian Mercury 400 spectrometer. Low resolution mass spectra were obtained using an ACQUITY triple quadrupole (TQD) low-resolution mass spectrometer (Waters Corp., USA) and high resolution mass spectra were obtained using a microTOFQ II ESI-Q-ToF LC/MS/MS system (Bruker Daltonics). Flash chromatography was performed on silica gel (200–300 mesh) and chromatographic solvent proportions are expressed as volume: volume. Stability was evaluated using an LC-10AVP high performance liquid chromatography system (Shimadzu, Japan). Reversed-phase chromatography was performed using an analytical Hedera ODS-2 column (4.6 × 250 mm, 5 µm). Uptake into rat primary hepatocytes was evaluated using an ACQUITY TQD mass spectrometer, equipped with a Z-spray ESI source and connected to an ACQUITY UPLC system. Samples were separated on a BEH C l8 column (2.1 × 50 mm, 1.7 µm), equipped with a Van Guard BEH C18 (2.1 × 5 mm, 1.7 µm, Waters Corp., USA) guard column. All anhydrous solvents were distilled from CaH$_2$ or Na/ benzophenone prior to use.

General procedure for synthesis of mono L-amino acid ester, mono bile acid ester prodrugs of adefovir (6a–f)

PMEA (0.47 mmol) and *N, N′*-dicyclohexyl-4-morpholine carboxamidine (DCMC) (0.94 mmol) were suspended in anhydrous DMF (40 mL) and stirred at 35–40 °C until the mixture become homogeneous. A solution of 3-bromo-1-propyl ester of deoxycholic acid (**3a**, 1.5 mmol) or 3-bromo-1-propyl ester of ursodesoxycholic acid (**3b**, 1.5 mmol) in anhydrous DMF (5 mL) was then added to the reaction solution and the mixtures were stirred at 40–50 °C for 48 h. Reaction processes were monitored by thin layer chromatography (TLC) (eluent: ethyl acetate/methanol 1:2 v/v) until generation of adefovir mono bile acid esters (**5a–b**) was judged to be at a maximum, although the products were not isolated from the mixture. Solutions of 3-bromo-1-propyl

esters of *N*-Boc L-amino acids (**4a–c**, 2.00 mmol) in anhydrous DMF (5 mL) were added to these solutions, and the reaction temperature was increased from 40–50 °C to 80–85 °C. After 48 h at 80–85 °C, the solvents were evaporated in vacuo. Ethyl acetate (50 mL) was then added to the residues and the mixtures were maintained at 4–6 °C for 12 h, filtered, and concentrated in vacuo. The residues were purified using flash column chromatography on silica gel (eluent: ethylacetate/methanol; 18:1–25:1, v/v) to provide mono *N*-Boc L-amino acid ester, mono bile acid ester prodrugs of adefovir.

A mixture of prodrug (0.45 mmol) and chloroform (3 mL) in a 25 mL flask was stirred at 0 °C until it became homogeneous. Aqueous phosphoric acid (60%, 1.5 mL, 15.35 mmol) was then added dropwise and the mixture was stirred vigorously. The reaction process was monitored by TLC (eluent: chloroform/methanol/formic acid 15:1:1 v/v) until the reaction was complete (4 h). Water (5 mL) and chloroform (5 mL) were then added and the mixture was neutralized (pH = 7.0) with saturated NaHCO$_3$ solution. The mixture was extracted three times with chloroform (50 mL) and the organic solution was dried over anhydrous MgSO$_4$, filtered, and evaporated in vacuo. The residue was purified by chromatography on silica gel (eluent: chloroform/methanol, 10:1–15:1, v/v), followed by preparative liquid phase chromatography using a CMB-20A instrument (Shimadzu, Japan). The samples were separated using an Agilent Prep-C18 column (30 × 250 mm, 10 µm). The elution gradient was: 30–100% MeOH-H$_2$O (0.01–10.00 min), 100–30% MeOH-H$_2$O (10.01–16.00 min), the mobile phase flow rate was 20 mL/min, the column temperature was 35 °C and the injection volume was 5 mL. Compounds (**6a–f**) were isolated by lyophilization using an FDU 1100 freeze drier (EYELA, Japan).
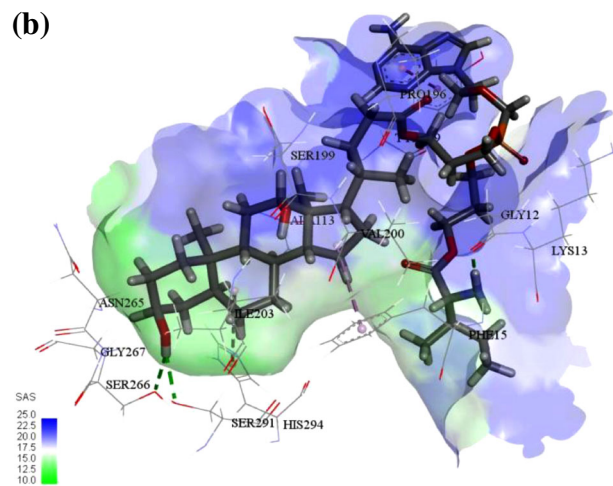
3-((((2-(6-amino-9H-purin-9-yl)ethoxy)methyl)(3-(((R)-2-aminopropanoyl)oxy)propoxy)phosphoryl)oxy)propyl 4-((3R,5S,7S,8R,9R,10S,13R,14S,17R)- 3,7-dihydroxy- 10,13-dimethylhexadecahydro-1H-cyclopenta[a]phenanthren-17-yl)pentanoate (6a):

Yield 14.5%, white foam solid. ^{1}H NMR (400MH, CDCl$_3$): δ 8.35(s, 1H, 2-H), 8.01(s, 1H, 8-H), 6.16(brs, 2H, NH$_2$), 4.45-4.42(m, 2H, NCH$_2$), 4.22-4.11(m, 7H, 2 × P(O)OCH$_2$, CH$_2$OCO, CHNH$_2$), 3.93(t, *J* = 4.0 Hz, 2H, NCH$_2$CH$_2$), 3.81(d, *J* = 8.0 Hz, 2H, OCH$_2$P), 3.71-3.68(m, 2H, CH$_2$OCO), 3.62-3.55(m, 2H, 2 × CHOH), 2.40-2.32(m, 1H), 2.26-2.19(m, 1H), 2.00-1.77(m, 16H), 1.70–1.41(m, 12H), 1.32–1.25(m, 8H), 0.94(s, 3H, CH$_3$), 0.93(d, *J* = 8.0 Hz, 6H, 2 × CH$_3$). ^{13}C NMR (100 MHz, CDCl$_3$): δ 174.41, 155.71, 153.01, 149.70, 141.58, 119.10, 71.32, 71.15, 65.72, 64.02, 63.59, 63.58, 63.51, 63.21, 63.20, 63.13, 60.24, 57.65, 55.86, 54.79, 43.75, 43.68, 43.48, 42.52, 40.19, 39.28, 37.34, 37.13, 35.26, 35.02, 34.12, 33.23,

(a)

Compound 6a

(b)
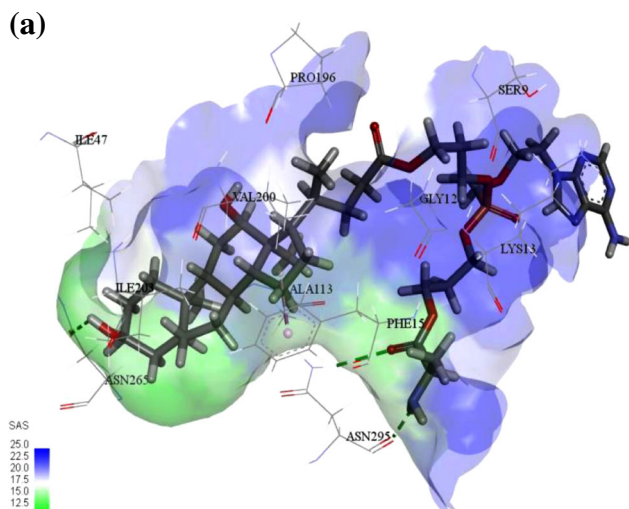
Compound 6c

Fig. 4 Proposed molecular binding modes of compounds **6a (a)** and **6c (b)** at the hASBT binding site (PDB code: 3ZUX). Color key: *Blue-green interface*, hASBT domain with *green* and *blue* depicting residues embedded in the protein and exposed to solvent, respectively; stick diagrams, *red*, oxygen atoms; *blue*, nitrogen atoms; *grey*, bile acid skeleton. *Green dashed lines* represent hydrogen bonds, *pink* and *purple dashed lines* indicate hydrophobic interactions between compounds and protein, respectively (color figure online)

31.18, 31.07, 30.34, 29.81, 28.73, 26.94, 23.48, 21.23, 18.46. ESI-MS (*m/z*) [M + H]$^+$: 835.3; HRESIMS *m/z* (pos): 835.4750 $C_{41}H_{68}$ $N_6O_{10}P$ (calcd. 835.4729).

3-(((3-(((R)-2-amino-3-methylbutanoyl)oxy)propoxy)((2-(6-amino-9H-purin-9-yl)ethoxy)methyl)phosphoryl)oxy)propyl 4-((3R,5S,7S,8R,9R,10S,13R,14S,17R)-3,7-dihydroxy-10,13-dimethylhexadecahydro-1H- cyclopenta[a] phenanthren-17-yl) pentanoate (6b):

Yield 17.8%, white foam solid. ^{1}H NMR (400MH, DMSO-d_6): δ 8.37(s, 1H, 2-H), 8.31 (s, 1H, 8-H), 4.53(t, *J* = 4.0 Hz, 2H, NCH$_2$),4.23(t, *J* = 8.0 Hz, 2H, NCH$_2$CH2), 4.14–4.06(m, 6H, CH$_2$OCO, 2 × P(O)OCH$_2$), 3.99–3.94(m, 5H, CH$_2$OCO, OCH$_2$P, CHNH$_2$), 3.48–3.43(m, 2H, 2 × CHOH), 2.40–2.30 (m, 1H), 2.26–2.20(m, 1H), 2.03–1.25(m, 30H), 1.07-1.04(m, 6H, 2 × CH$_3$), 0.95–0.92(m, 9H, 3 × CH$_3$); ^{13}C NMR (100 MHz, DMSO-d_6):δ 174.19, 168.65, 152.27, 149.41, 146.94, 144.08, 118.40, 70.76, 70.59, 64.43, 63.48, 63.08, 62.84, 62.00, 60.16, 58.05, 57.02, 56.14, 55.12, 53.50, 43.52, 43.42, 43.14, 42.67, 40.20, 39.35, 37.26, 36.62, 35.33, 34.73, 33.83, 30.92, 30.68, 29.66, 29.46, 29.21, 28.36, 26.61, 22.59, 21.03, 17.59, 17.36, 16.91. ESI-MS (*m/z*) [M + H]$^+$: 863.6; HRE-SIMS *m/z* (pos):863.5043 $C_{43}H_{72}N_6O_{10}P$ (calcd. 863.5042).

(2R)-3-((((2-(6-amino-9H-purin-9-yl)ethoxy)methyl)(3-((4-((3R,5S,7S,8R,9R,10S,13R,14S,17R)-3,7-dihydroxy-10,13-dimethylhexadecahydro-1H-cyclopenta[a]phenanthren-17-

yl)pentanoyl)oxy)propoxy)phosphoryl)oxy)propyl 2-amino-3- methyl pentanoate (6c):

Yield 19.7%, light yellow foam solid. ^{1}H NMR (400MH, CDCl$_3$): δ 8.28(s, 1H, 2-H), 7.94 (s, 1H, 8-H), 6.36(brs, 2H, NH$_2$),4.41(t, *J* = 8.0 Hz, 2H, NCH$_2$), 4.22–4.07(m, 9H, 2 × P (O)OCH$_2$, 2 × CH$_2$OCO, CHNH$_2$), 3.92(t, *J* = 8.0 Hz, 2H, NCH$_2$C*H*$_2$), 3.79(d, *J* = 8.0 Hz, 2H, OCH$_2$P), 3.59-3.53 (m,2H, 2 × CHOH), 2.37–2.29(m, 1H), 2.23–2.17(m, 1H), 1.97–1.15(m, 48H); ^{13}CNMR (100 MHz, CDCl$_3$):δ 174.29, 155.54, 152.73,149.76, 141.55, 119.07, 71.44, 71.28, 65.83, 65.80, 64.17, 63.24, 63.18, 62.98, 62.93, 62.86, 60.94, 60.90, 60.22, 58.47, 55.84, 54.90,50.84, 43.78, 42.52, 40.20, 39.28, 37.35, 37.00, 35.29, 35.01, 34.13, 31.12, 30.39, 29.79, 28.74, 26.94, 24.80, 23.46, 22.94, 21.95, 21.23, 18.46, 12.19. ESI-MS (*m/z*) [M + H]$^+$: 878.0; HRESIMS *m/z* (pos): 877.5205 $C_{44}H_{74}$ $N_6O_{10}P$ (calcd. 877.5199).

3-((((2-(6-amino-9H-purin-9-yl)ethoxy)methyl)(3-(((R)-2-aminopropanoyl)oxy)propoxy)phosphoryl)oxy)propyl 4-((3R,5R,8R,9R,10S,12S,13R,14S,17R)- 3,12-dihydroxy-10,13-dimethylhexadecahydro-1H-cyclopenta[a] phenanthren-17-yl)pentanoate (6d):

Yield 21.8%, light yellow oil. ^{1}H NMR (400MH, CDCl$_3$): δ 8.26(s, 1H, 2-H), 7.99(s, 1H, 8-H), 6.57(brs, 2H,NH$_2$), 4.39-4.38(m, 2H, NCH$_2$), 4.15–4.06(m, 6H, 2 × P(O) OCH$_2$, CH$_2$OCO), 3.96(m, 1H, CHNH$_2$), 3.89-3.86(m, 2H, NCH$_2$CH$_2$), 3.82(d, *J* = 8.0 Hz, 2H, OCH$_2$P), 3.65–3.61(m, 2H, CH$_2$OCO), 3.57–3.51(m, 2H, 2 × CHOH), 2.35–2.29(m,

1H), 2.24-2.20(m, 1H), 1.93–1.90(m, 2H, CH_2CO), 1.80-0.94 (m, 33H), 0.85–0.82(m, 6H); ^{13}C NMR (100 MHz, $CDCl_3$):δ 174.56, 174.51, 155.77, 153.03, 149.7, 141.72, 141.56, 118.96, 73.08, 71.58, 71.14, 65.65, 64.01, 63.63, 63.55, 63.48, 63.24, 63.18, 63.15, 63.08, 60.17, 57.66, 48.39, 46.69, 46.63, 43.52, 42.09, 36.37, 35.35, 34.18, 33.64, 30.90, 29.80, 28.60, 27.69, 27.08, 26.23, 23.75, 23.16, 17.32, 17.25. ESI-MS (m/z) $[M + H]^+$: 835.3; HRESIMS m/z (pos): 835.4743 $C_{41}H_{68}N_6O_{10}P$ (calcd. 835.4729).

3-(((3-(((R)-2-amino-3-methylbutanoyl)oxy)propoxy)((2-(6-amino-9H-purin-9-yl)ethoxy)methyl)phosphoryl)oxy)propyl 4-((3R,5R,8R,9R,10S,12S,13R,14S,17R)- 3,12- dihydroxy-10,13-dimethylhexadecahydro-1H-cyclopenta[a] phenanthren-17-yl)pentanoate (6e):

Yield 20.6%, light yellow foam solid. ^{1}H NMR (400MH, $CDCl_3$): δ 8.31(s, 1H, 2-H), 7.99(s, 1H, 8-H), 6.60(brs, 2H, NH_2), 4.43(t, $J = 4.4$ Hz, 2H, NCH_2), 4.20–4.08(m, 8H, $2 \times CH_2OCO$, $2 \times P(O)OCH_2$), 4.01(m, 1H, $CHNH_2$), 3.95-3.92 (m, 2H, NCH_2CH_2), 3.82(d, $J = 8.0$ Hz, 2H, OCH_2P), 3.64–3.57(m, 2H, $2 \times CHOH$), 2.39–2.33(m, 1H), 2.26–2.21 (m, 1H), 2.04–1.96(m, 6H), 1.86–1.22(m, 26H), 1.00–0.96 (m, 9H, $3 \times CH_3$), 0.91–0.89(m, 6H, $2 \times CH_3$); ^{13}C NMR (100 MHz, $CDCl_3$):δ 174.22, 172.67, 155.92, 152.85, 149.63, 141.29, 118.99, 72.94, 72.89, 71.44, 71.12, 66.54, 63.22, 63.17, 63.13, 62.94, 62.87, 61.99, 61.36, 60.65, 60.43, 60.38, 58.20, 55.81, 54.93, 46.50, 43.71, 42.49, 40.15, 39.21, 37.65, 35.27, 34.07, 30.23, 29.68, 28.64, 25.03, 23.45, 21.19, 19.25, 18.40, 17.33, 15.56. ESI-MS (m/z) $[M + H]^+$: 863.8; HRE-SIMS m/z (pos): 863.5052 $C_{43}H_{72}N_6O_{10}P$ (calcd. 863.5042).

(2R)-3-((((2-(6-amino-9H-purin-9-yl)ethoxy)methyl)(3-((4-((3R,5R,8R,9R,10S,12S,13R,14S,17R)-3,12-dihydroxy-10,13-dimethylhexadecahydro-1H-cyclopenta[a] phenanthren-17-yl)pentanoyl)oxy)propoxy)phosphoryl)oxy) propyl 2-amino-3- methyl- pentanoate (6f):

Yield 16.7%, colorless oil. ^{1}H NMR (400MH, DMSO-d_6): δ 8.23(s, 1H, 2-H), 7.92 (s, 1H, 8-H), 4.48(t, $J = 4.0$ Hz, 2H, NCH_2), 4.35–4.25(m, 2H, CH_2OCO, $CHNH_2$), 4.12–4.04 (m, 6H, $2 \times P(O)OCH_2$, CH_2OCO), 3.98-3.93(m, 3H, $CHNH_2$, NCH_2CH2), 3.56–3.48(m, 2H, $2 \times CHOH$), 2.41–2.34(m, 1H), 2.28–2.20(m, 1H), 2.00–1.24(m, 38H), 1.03–0.87(m, 12H, $4 \times CH_3$). ^{13}C NMR (100 MHz, DMSO-d_6):δ 175.01, 174.16, 155.47, 152.92, 149.76, 141.34, 119.12, 71.33, 71.16, 65.77, 64.10, 64.06, 63.11, 63.04, 62.86, 60.59, 60.11, 58.91, 55.73, 54.69, 50.73, 43.68, 43.55, 42.41, 40.08, 39.15, 37.25, 36.89, 35.17, 34.90, 34.02, 31.01, 30.29, 29.75, 29.67, 29.34, 28.63, 26.82, 24.77, 23.55, 21.12, 18.35, 15.65, 12.09. ESI-MS (m/z) $[M + H]^+$: 877.8; HRESIMS m/z (pos): 877.5192 $C_{44}H_{74} N_6O_{10}P$ (calcd. 877.5199).

Anti-HBV activity of compounds 6a–f

The effect of the compounds on HIV replication was evaluated in HepG2 2.2.15 cells, according to the method described by Sells (Sells et al. 1987). HepG2.2.2.15 cells were plated at a density of 5×10^4 cells/well on 96-well plates and incubated for 2 days. The medium was then replaced by medium containing the test compounds in gradient concentration (10, 1, 0.1 mg/mL). After 2 days treatment, the culture medium was removed and fresh medium containing the same concentration of the test compound was added to the culture. At day 10, the supernatants were collected and lysed for analysis of intracellular HBV DNA. The amount of HBV DNA at each concentration was measured by real time PCR using an Icycler real-time PCR Detection System (Bio-Rad). Amplification primers were HBVFP: 5'-TGT CCT GGTTAT CGC TGG-3' and HBVRP: 5'-CAA ACG GGC AAC ATA CCT T-3'.The TaqMan probe was FAM-5'-TGT GTC TGC GGC GTT TTA TCAT-3' -TAMRA. Half maximum cytotoxic concentration (CC_{50}) values for each compound were measured by calculating cell growth rates using a standard procedure. The cells were plated at a density of 5×10^4 cells/well on 96-well plates and incubated for 12 h. The supernatant was then replaced with Dulbecco's modified Eagle medium containing the test compound with final concentrations of 1000, 100, and 10 μM, and the cells were cultured for 2 more days. At the end of the incubation period, Cell Counting Kit-8 (CCK-8, 100 μL) was added to the wells and the cells were cultured for a further 2 h. OD values were measured at 450 nm. The data were analyzed using Icycler IQ 3.0 software. EC_{50}, CC_{50}, and SI of the test compounds are provided in Table 1. AD was used as a positive control.

Uptake of compounds 6a–f in rat primary hepatocytes

The uptake of compounds **6a–f**, which had improved antiviral activity and stability, was evaluated in rat primary hepatocytes, using AD as a positive control. The cells were isolated from the liver of overnight-fasted Sprague-Dawley rats using the two step collagenase perfusion method (La Brecque and Howard 1976). Cell viability was tested using the trypan blue dye exclusion test within 1 h of isolation. Hepatocytes were maintained in RPMI-1640 medium, supplemented with heat-inactivated fetal bovine serum (FBS) (10%)(Gibco Life Technologies), penicillin (50 units/mL), streptomycin (50 mg/mL) and geneticin (1 mg/mL), under an atmosphere of 5% CO_2-95% air in a Thermo Forma 371 incubator, with humidity controlled at 37 °C. Liver cell-specificity was characterized using a CK18 immunohistochemical kit (IHC kits) and cell preparations with viability > 95% were used for the experiments. RPMI-1640 media containing AD or compounds **6a–f** (50 μM) was added to cultured primary rat hepatocytes

on six-well plates, and the cells were grown at 37 °C in a humidified incubator with an atmosphere of 5% CO_2. Cells were withdrawn after 5, 15, 30, and 60 min cultivation and washed three times with D-Hanks solution at 4 °C. Radio-immunoprecipitation assay (RIPA) buffer (250 μL) was then added to lyse the cells. The cell lysis solution was then centrifuged at 13,000 × g for 20 min at 4 °C and an aliquot of supernatant (20 μL) was withdrawn for determination of protein levels using a BCA protein assay kit (Thermo Scientific Pierce, NCI3225CH). In a second experiment, methanol (800 μL) was added to cell lysis solution (200 μL) and the mixed solution was centrifuged twice at 13,800 × g for 20 min at 4 °C to precipitate proteins. An aliquot of the supernatant solution (20 μL) was assayed using the established UPLC-MS/MS analytical method. The inhibitory effect of deoxycholic acid (100 μM) on uptake of compounds 6a–f byprimary hepatocytes was also evaluated to ascertain whether active transport by bile acid carrier was involved in uptake of the compounds.

Liquid chromatography/tandem mass spectrometry (UPLC-MS/MS) analysis conditions: UPLC analyses were performed using an ACQUITY UPLC instrument (Waters Corp.). The samples were separated on a BEH C l8 column (2.1 × 50 mm, 1.7 μm), equipped with a Van Guard BEH C18 (2.1 × 5 mm, 1.7 μm, Waters Corp.) guard column. The mobile phase consisted of acetonitrile containing 0.1% formic acid (A) and water containing 0.1% formic acid (B). The elution gradient was: 5% A (0–3.5 min), 100% A (3.5–4.0 min), 5% A (4.0–5.0 min). The mobile phase flow rate was 0.35 mL/min, and the column temperature was set at 45 °C. The injection volume for the hepatocyte uptake assay was 2 μL. Mass spectrometry identifications were carried out using an ACQUITY TQD mass spectrometer, equipped with a Z-spray ESI source and connected to an ACQUITY UPLC system. The acquisition parameters were: collision gas, argon (Ar); nebulizing and drying gas, nitrogen (N_2); source temperature, 120 °C; desolvation temperature, 350 °C; cone gas flow rate, 50 L/h; desolvation gas flow rate, 650 L/h; collision gas flow rate, 0.16 mL/min; and capillary voltage, 3.0 kV. Selected ion monitoring mode was used. In positive ion mode (ESI^+), the confirmation ion pairs were (m/z): 501.1 (AD), 835.1 (6a), 863.2 (6b), 877.1 (6c), 835.1 (6d), 863.1(6e), and 877.2 (6f) and the cone voltage was 40 V. The results are summarized in Figs. 1 and 2.

Uptake of compounds 6a–f in NTCP-Hek293 cells

Cell culture

HEK cells were cultured at 37 °C with 90% humidity and 5% CO_2, as previously described (Leonhardt et al. 2010). Cells were fed every 2 days with Dulbecco's modified eagle medium, supplemented with FBS (10%), penicillin (50 units/mL), streptomycin (50 mg/mL), non-essential amino acids (1%) and geneticin (1 mg/mL) to maintain selection pressure. Cells were passaged approximately every 4 days Leonhardt et al. (2010).

Transfection

NTCP cDNA (GenBank accession no. L21893.1) was amplified by PCR (Bio-Rad). The sequences of the forward and reverse primers used to obtain full-length NTCP cDNA were 5′-GGTCCTGGTTCTCATTCCT-3′ and 5′-AGAG-TAATATCATGGCAAA-3′. Coding sequences of the transporters were cloned into vector pEGFP-N1 (Biomed, Beijing, China). The NTCP-cloned vector was then characterized by digestion with EcoR I and BamH I (Thermo Fisher Scientific) (Kullak–Ublick et al. 2000). The NTCP constructs were transiently transfected into HEK293 cells using FuGENE6, according to the manufacturer's instructions. Briefly, when 90% confluent, cells were seeded at a density of $2.4 × 10^5$ cells/well in six-well plates and transfections were performed on day 2 after seeding. DNA and FuGENE 6 (1:3 DNA-FuGENE 6) were combined in serum-free medium and added to each well. Transfected cells were incubated for 30 h. The transfected cells were characterized by RT-PCR and western blot analysis (Maeda et al. 2006).

Uptake into NTCP-HEK cells

Donor solutions contained 10, 25, 50, 100 or 200 μmol L^{-1} taurocholate and AD or compounds 6a–f in either Hank's balanced salt solution containing sodium chloride (137 mM, pH 6.8) (to measure total uptake) or sodium-free buffer, in which sodium chloride was replaced by tetraethylammonium chloride (137 mM, pH 6.8) (to measure Na^+-independent, passive uptake). After incubation at 37 °C for 30 min (Vivian and Polli 2014), the cells were lysed with RIPA buffer. The cell lysis solution was then centrifuged at 13,000 × g for 20 min at 4 °C. An aliquot (20 μL) of the supernatant was withdrawn for determination of protein levels using a BCA Protein Assay Kit (Thermo Scientific Pierce, NCI3225CH). In a second experiment, cell lysis solution (200 μL) was treated with methanol (800 μL) and the mixture was centrifuged twice at 13,800 × g for 20 min at 4 °C to precipitate protein. Analysis by UPLC-MS/MS was performed using the same conditions as those used in the rat primary hepatocyte uptake studies. During each determination of prodrug uptake, the V_{max} oftaurocholate was measured to normalize NTCP expression. Prodrug V_{max} was divided by taurocholate V_{max} to provide normalized V_{max} values for the prodrug. Prodrug kinetic parameters, K_m and V_{max}, were determined using Eadie–Hofstee plots and taurocholate and test compounds 6a–f all appear to show saturable kinetics. Michaelis–Menten constants (K_m) and V_{max} were calculated using the following equation: $y = V_{max} × x/(K_m + x)$.

Molecular docking

A docking analysis was carried out using C-DOCKER module (Discovery Studio, version 4.0; Accelrys, San Diego, CA, USA, 2008) to compare the binding modes of compounds **6a** and **6c** bound to hASBT. The X-ray crystallographic structure of hASBT (PDB ID: 3ZUY) was used for the docking calculations. After removing the ligand and water molecules, the CHARMm-force field was applied to the protein. The hASBT binding pocket was chosen as the active site, with the radius set at 8 Å. Random ligand conformations were generated using CHARMm-based molecular dynamics (1000 steps) and these were then docked into the defined hASBT binding site. Other parameters were set to default values. The final binding conformations of **6a** and **6c** were determined using the calculated docking energy. The most stable binding modes among the top 10 docking poses of **6a** and **6c** are presented in Fig. 4a and b, respectively.

Compliance with ethical standards

Conflict of interest The authors declare that they have no competing interests.

References

Bader A, Borel Rinkes IH, Closs EI, Ryan CM, Toner M, Cunningham JM, Tompkins RG, Yarmush ML (1992) A stable long-term hepatocyte culture system for studies of physiologic processes: cytokine stimulation of the acute phase response in rat and human hepatocytes. Biotechnol Prog 8:219–225

Balakrishnan A, Polli JE (2006) Apical sodium dependent bile acid transporter (ASBT, SLC10A2): a potential prodrug target. Mol Pharm 3:223–230

Dunn JC, Yarmush ML, Koebe HG, Tompkins RG (1989) Hepatocyte function and extracellular matrix geometry: long-term culture in a sandwich configuration. FASEB J 3:174–177

Fiorucci S, Antonelli E, Brancaleone V, Sanpaolo L, Orlandi S, Distrutti E, Acuto G, Clerici C, Baldoni M, Del Soldato P, Morelli A (2003) NCX-1000, a nitric oxide-releasing derivative of ursodeoxycholic acid, ameliorates portal hypertension and lowers norepinephrine-induced intrahepatic resistance in the isolated and perfused rat liver. J Hepatol 39:932–939

Fu XZ, Jiang SH, Li C, Xin J, Yang YS, Ji RR (2007) Design and synthesis of novel bis(L-amino acid) ester prodrugs of 9-[2-(phosphonomethoxy)ethyl]adenine (PMEA) with improved anti-HBV activity. Bioorg Med Chem Lett 17:465–470

Fu XZ, Ou Y, Pei JY, Liu Y, Li J, Zhou W, Lan YY, Wang AM, Wang YL (2012) Synthesis, anti-HBV activity and renal cell toxicity evaluation of mixed phosphonate prodrugs of adefovir. Eur J Med Chem 49:211–218

Fung J, Lai CL, Yuen MF (2008) LB80380: a promising new drug for the treatment of chronic hepatitis B. Expert Opin Investig Drugs 17:1581–1588

Gitlin N (1997) Hepatitis B: diagnosis, prevention, and treatment. Clin Chem 43:1500–1506

Jarvis B, Faulds D (1999) Lamivudine. A review of its therapeutic potential in chronic hepatitis B. Drugs 58:101–141

Kullak-Ublick GA, Glasa J, Böker C, Oswald M, Grützner U, Hagenbuch B, Stieger B, Meier PJ, Beuers U, Kramer W, Wess G, Paumgartner G (1997) Chlorambucil-taurocholate is transported by bile acid carriers expressed in human hepatocellular carcinomas. Gastroenterology 113:1295–1305

La Brecque DR, Howard RB (1976) The preparation and characterization of intact isolatedparenchymal cells from rat liver. Methods Cell Biol 14:327–340

Leonhardt M, Keiser M, Oswald S, Kühn J, Jia J, Grube M, Kroemer HK, Siegmund W, Weitschies W (2010) Hepatic Uptake of the Magnetic Resonance Imaging Contrast Agent Gd-EOB-DTPA: Role of Human Organic Anion Transporters. Drug Metab Dispos 38 (7):1024–1028

Kullak-Ublick GA, Ismair MG, Kubitz R, Schmitt M, Häussinger D, Stieger B, Hagenbuch B, Meier PJ, Beuers U, Paumgartner G (2000) Expression and functional characterization of a Na$^+$-taurocholate cotransporting green fluorescent protein in human hepatoblastoma HepG2 cells. Cytotechnology 34:1–9

Kullak-Ublick GA, Stieger B, Meier PJ (2004) Enterohepatic bile salt transporters in normal physiology and liver disease. Gastroenterology 126:322–342

Law ST, Li KK, Ho YY (2013) Acquired fanconi syndrome associated with prolonged Adefovir Dipivoxil therapy in a chronic hepatitis B patient. Am J Ther 20:713–716

Maeda K, Kambara M, Tian Y, Hofmann AF, Sugiyama Y (2006) Uptake of ursodeoxycholate and its conjugates by human hepatocytes: Role of Na(+)-taurocholatecotransporting polypeptide (NTCP), organic anion transporting polypeptide (OATP) 1B1 (OATP-C), andoatp1B3 (OATP8). Mol Pharm 3:70–77

Quan DJ, Peters MG (2004) Antiviral therapy: nucleotide and nucleoside analogs. Clin Liver Dis 8:371–385

Rais R, Fletcher S, Polli JE (2011) Synthesis and in vitro evaluation of gabapentin prodrugs that target the human apical sodium-dependent bile acid transporter (hASBT). J Pharm Sci 100:1184–1195

Raney AK, Hamatake RK, Hong Z (2003) Agents in clinical development for the treatment of chronic hepatitis B. Expert Opin Investig Drugs 12:1281–1295

Revill P, Locarnini S (2016) Antiviral strategies to eliminate hepatitis B virus covalently closed circular DNA (cccDNA). Curr Opin Pharmacol 30:144–150

Schaap FG, Trauner M, Jansen PL (2014) Bile acid receptors as targets for drug development. Nat Rev Gastroenterol Hepatol 11:55–67

Sells MA, Chen ML, Acs G (1987) Production of hepatitis B virus particles in Hep G2 cells transfected with cloned hepatitis B virus DNA. Proc Natl Acad Sci USA 84:1005–1009

Valle R, Haragsim L (2006) Nephrotoxicity as a complication of antiretroviral therapy. Adv Chronic Kidney Dis 13:314–319

Vicens M, Medarde M, Macias RI, Larena MG, Villafaina A, Serrano MA, Marin JJ (2007) Novel cationic and neutral glycocholic acid and polyamine conjugates able to inhibit transporters involved in hepatic and intestinal bile acid uptake. Bioorg Med Chem 15:2359–2367

Vivian D, Polli JE (2014) Synthesis and in vitro evaluation of bile acid prodrugs of floxuridine to target the liver. Int J Pharm 475:597–604

You H, Jia J (2013) Telbivudine treatment in chronic hepatitis B: experience from China. J Viral Hepat Suppl 1:3–8

Yuen MF, Lai CL (2004) Adefovir dipivoxil in chronic hepatitis B infection. Expert Opin Pharmacother 5:2361–2367